

A Test of $f(Q, C)$ Gravity Model with Application to the Photometric Maximum

Lorenzo Zaninetti

Physics Department, University of Turin, Turin, Italy

Email: l.zaninetti@alice.it

How to cite this paper: Zaninetti, L. (2025) A Test of $f(Q, C)$ Gravity Model with Application to the Photometric Maximum. *Journal of High Energy Physics, Gravitation and Cosmology*, 11, 1333-1351. <https://doi.org/10.4236/jhepgc.2025.114083>

Received: June 21, 2025

Accepted: September 23, 2025

Published: September 26, 2025

Copyright © 2025 by author(s) and Scientific Research Publishing Inc. This work is licensed under the Creative Commons Attribution International License (CC BY 4.0).

<http://creativecommons.org/licenses/by/4.0/>



Open Access

Abstract

We review the $f(Q, C)$ gravity with its three models for the equation of state (EoS). We introduce three new models for the EoS and we derive the parameters of these six models from the Pantheon+ catalog. The comparison of the results is done with the dynamical dark energy cosmology and the standard cosmology or Λ CDM. The results are applied to the photometric maximum in the number of galaxies as a function of the redshift.

Keywords

Galaxy Groups, Clusters, and Superclusters, Large Scale Structure of the Universe Cosmology

1. Introduction

The number of supernovae (SNs) of type Ia for which the distance modulus is available has grown with time: 34 SNs in the sample which produced evidence for the accelerating universe [1], 580 SNs in the Union 2.1 compilation [2], 740 SNs in the joint light-curve analysis (JLA) [3], 1048 SNs in the Pantheon sample [4] [5] and 1701 SNs in the Pantheon+ sample [6]. The increase in the number of elements in the catalogs of distance modulus for type Ia supernovae (SNe Ia) allows testing various old cosmological theories as well as the new ones. As an example in the framework of the Pantheon+ sample [6], the following existing cosmologies were analysed: the Flat Λ CDM model and the Flat w_0 CDM model. An example of a new type of cosmology is represented by the $f(Q, C)$ gravity where Q and C stand for the non-metricity scalar and boundary term [7]. This first model in $f(Q, C)$ gravity was followed by an astronomically oriented paper [8] in which the three parameters of the theory were derived by analysing the distance modulus for supernovae as given by the Pantheon sample. The present paper pre-

sents, in Section 2, the standard knowledge for two popular cosmologies and Section 3 reviews the basic equations of the $f(Q, C)$ gravity. Section 4 derives the three astrophysical parameters for the six models of the $f(Q, C)$ gravity and Section 5 applies the $f(Q, C)$ gravity to model the maximum in the number of galaxies as a function of the redshift.

2. Two Standard Cosmologies

We will now review the Λ CDM and the wCDM cosmologies.

2.1. The Standard Cosmology

In Λ CDM cosmology, the *Hubble distance* D_H is defined by

$$D_H \equiv \frac{c}{H_0}, \quad (1)$$

where c is the speed of light and H_0 is the Hubble constant. We then introduce a parameter Ω_M

$$\Omega_M = \frac{8\pi G \rho_0}{3H_0^2}, \quad (2)$$

where G is the Newtonian gravitational constant and ρ_0 is the mass density at the present time. Another is Ω_Λ

$$\Omega_\Lambda \equiv \frac{\Lambda c^2}{3H_0^2}, \quad (3)$$

where Λ is the cosmological constant, see [9]. Once Ω_Λ and H_0 are set, the numerical value of the cosmological constant is derived, $\Lambda \approx 1.2 \frac{1}{\text{m}^2}$.

The two previous parameters are connected with the curvature Ω_K by

$$\Omega_M + \Omega_\Lambda + \Omega_K = 1. \quad (4)$$

The comoving distance, D_C , is

$$D_C = c \int_0^z \frac{dz'}{E(z')}, \quad (5)$$

where c is the speed of light and $E(z)$ is the ‘‘Hubble function’’

$$E(z) = \sqrt{\Omega_M (1+z)^3 + \Omega_K (1+z)^2 + \Omega_\Lambda}. \quad (6)$$

The above integral cannot be done in analytical terms, except for the case of $\Omega_\Lambda = 0$, but the Padé approximant, see Appendix A in [10], allows us to derive an approximation for the indefinite integral.

The approximate definite integral for (5) is therefore

$$D_{C,2,2} = D_H \left(F_{2,2}(z; a_0, a_1, a_2, b_0, b_1, b_2) - F_{2,2}(0; a_0, a_1, a_2, b_0, b_1, b_2) \right), \quad (7)$$

where $F_{2,2}$ is from equation (A10) in [10]. The transverse comoving distance D_M is

$$D_M = \begin{cases} D_H \frac{1}{\sqrt{\Omega_K}} \sinh \left[\sqrt{\Omega_K} D_C / D_H \right] & \text{for } \Omega_K > 0 \\ D_C & \text{for } \Omega_K = 0 \\ D_H \frac{1}{\sqrt{|\Omega_K|}} \sin \left[\sqrt{|\Omega_K|} D_C / D_H \right] & \text{for } \Omega_K < 0 \end{cases} \quad (8)$$

The approximate transverse comoving distance, $D_{M,2,2}$, computed with the Padé approximant, is

$$D_{M,2,2} = \begin{cases} D_H \frac{1}{\sqrt{\Omega_K}} \sinh \left[\sqrt{\Omega_K} D_{C,2,2} / D_H \right] & \text{for } \Omega_K > 0 \\ D_{C,2,2} & \text{for } \Omega_K = 0 \\ D_H \frac{1}{\sqrt{|\Omega_K|}} \sin \left[\sqrt{|\Omega_K|} D_{C,2,2} / D_H \right] & \text{for } \Omega_K < 0 \end{cases} \quad (9)$$

The Padé approximant for the luminosity distance is

$$D_{L,2,2} = (1+z) D_{M,2,2}, \quad (10)$$

and the Padé approximant for the distance modulus, $(m-M)_{2,2}$, is

$$(m-M)_{2,2} = 25 + 5 \log_{10} (D_{L,2,2}). \quad (11)$$

2.2. Dynamical Dark Energy or wCDM

In the dynamical dark energy cosmology (wCDM), first introduced by [11], the *Hubble distance* is

$$D_H(z; \Omega_M, w, \Omega_{DE}) = \frac{1}{\sqrt{(1+z)^3 \Omega_M + \Omega_{DE} (1+z)^{3+3w}}}, \quad (12)$$

where w is the equation of state, here considered constant, see equation (3.4) in [12] or equation (18) in [13] for the luminosity distance. Here we assumed w to be constant but also the case of w as a function of z can be considered, see equation (19) in [13]. In the above cosmology, the cosmological constant is absent. In flat cosmology,

$$\Omega_M + \Omega_{DE} = 1, \quad (13)$$

and the *Hubble distance* becomes

$$D_H(z; \Omega_M, w) = \frac{1}{\sqrt{(1+z)^3 \Omega_M + (1-\Omega_M)(1+z)^{3+3w}}}. \quad (14)$$

The indefinite integral in the variable z of the above *Hubble distance*,

$I_z \equiv \frac{D_C}{D_H}$, is

$$I_z(z; \Omega_M, w) = \int D_H(z; \Omega_M, w) dz, \quad (15)$$

where the new symbol I_z underlines the mathematical operation of integration. In order to obtain the indefinite integral, we perform a change of variable $1+z = t^{1/3}$

$$I_z(t; \Omega_M, w) = \frac{1}{3} \int \frac{1}{\sqrt{-t((-1 + \Omega_M)t^w - \Omega_M)} t^{2/3}} dt. \tag{16}$$

The indefinite integral is

$$I_z(t; \Omega_M, w) = \frac{-2 {}_2F_1\left(\frac{1}{2}, -\frac{1}{6} w^{-1}; 1 - \frac{1}{6} w^{-1}; -\frac{t^w - (1 - \Omega_M)}{\Omega_M}\right)}{\sqrt{\Omega_M} \sqrt[6]{t}}, \tag{17}$$

where ${}_2F_1(a, b; c; z)$ is the regularized hypergeometric function, see [14]-[18]. We now return to the variable z , the redshift and then the indefinite integral becomes

$$I_z(z; \Omega_M, w) = \frac{-2 {}_2F_1\left(\frac{1}{2}, -\frac{1}{6} w^{-1}; 1 - \frac{1}{6} w^{-1}; -\frac{(-z^3 + 3z^2 + 3z + 1)^w (1 - \Omega_M)}{-\Omega_M}\right)}{\sqrt{\Omega_M} \sqrt[6]{z^3 + 3z^2 + 3z + 1}}. \tag{18}$$

We denote by $F(z; \Omega_M, w)$ the definite integral

$$F(z; \Omega_M, w) = I_z(z; \Omega_M, w) - I_z(z = 0; \Omega_M, w). \tag{19}$$

The luminosity distance, D_L , for Λ CDM cosmology in the case of the analytical solution is

$$D_L(z; c, H_0, \Omega_M, w) = \frac{c}{H_0} (1 + z) F(z; \Omega_M, w), \tag{20}$$

where $F(z; \Omega_M, w)$ is given by Equation (19) and the distance modulus is

$$(m - M) = 25 + 5 \log_{10}(D_L(z; c, H_0, \Omega_M, w)). \tag{21}$$

More details can be found in [19].

3. The $f(Q, L_m)$ Gravity Model

We review the current results of the $f(Q, L_m)$ cosmology and the methods of integrating the Hubble function. The three existing models are presented and another three models are added.

3.1. The New Cosmology

We are interested in the astrophysical applications of the $f(Q, L_m)$ gravity model as presented in [8]. The basic astrophysical parameter is ω , which represents the equation of state (EoS) of dark matter. The comoving distance, D_C , is

$$D_C = c \int_0^z \frac{dz'}{E(z')}, \tag{22}$$

where $E(z)$ is the ‘Hubble function’ and the luminosity distance is

$$D_L = (1 + z) D_C. \tag{23}$$

The distance modulus $\mu(z)$ is

$$\mu(z) = (m - M) = 25 + 5 \log_{10} \left(D_L(z; c, H_0, w) \right), \quad (24)$$

where m and M are the apparent and absolute magnitude. In the $f(Q, L_m)$ gravity model three models are presented.

3.2. How to Integrate the Hubble Function

The definite integral, which represents the ‘‘Hubble function’’, can be evaluated in the following different ways:

- 1) analytical integration;
- 2) numerical integration;
- 3) approximate integration using a series for the integrand;
- 4) approximate integration using a Padé approximant $R_{k,l}(x) = p(x)/q(x)$ for the integrand where $p(x)$ is a polynomial of degree k and $q(x)$ is a polynomial of degree l .

3.3. First Model

The first model is a linear dependence for the EoS

$$\omega = z\omega_1 + \omega_0, \quad (25)$$

which corresponds to

$$H(z) = H_0 (1+z)^{\frac{3\omega_0}{2} + \frac{3}{2}} \frac{3\omega_1}{2} e^{\frac{3z\omega_1}{2}}. \quad (26)$$

In this case, the integral (22) can be evaluated and is

$$D_C = \frac{N}{A}, \quad (27)$$

where

$$\begin{aligned} N = & - \left(\Gamma \left(-\frac{3\omega_0}{2} + \frac{3\omega_1}{2} + \frac{3}{2}, \frac{3\omega_1(1+z)}{2} \right) \right. \\ & \left. - \Gamma \left(-\frac{3\omega_0}{2} + \frac{3\omega_1}{2} + \frac{3}{2}, \frac{3\omega_1}{2} \right) \right) e^{\frac{3\omega_1}{2} \frac{1}{\omega_1^2} + \frac{3\omega_0}{2} \frac{3\omega_1}{2}} \sqrt{1+z} 3^{2+\frac{3\omega_0}{2}} \frac{3\omega_1}{2} \frac{3\omega_0}{2} \frac{3\omega_1}{2} + \frac{3}{2} \\ & + 6(1+z)^{-\frac{3\omega_0}{2} + \frac{3\omega_1}{2}} e^{-\frac{3\omega_1 z}{2}} \left((2+z)\omega_1 - \omega_0 + \frac{1}{3} \right) + 6\sqrt{1+z} \left(\omega_0 - 2\omega_1 - \frac{1}{3} \right), \end{aligned} \quad (28)$$

and

$$A = \sqrt{1+z} (1+3\omega_0 - 3\omega_1) (-1+3\omega_0 - 3\omega_1) H_0, \quad (29)$$

where $\Gamma(a, z)$ is the incomplete Gamma function defined by

$$\Gamma(a, z) = \int_z^\infty t^{a-1} e^{-t} dt, \quad (30)$$

see [18]. The luminosity distance is given by Equation (23) and its derivative with respect to the redshift is

$$\begin{aligned} \frac{\partial D_L}{\partial z} = & \frac{1}{\sqrt{1+z}(1+3\omega_0-3\omega_1)(-1+3\omega_0-3\omega_1)H_0} \\ & \times 2c \left(\omega_1^2 \frac{1+3\omega_0-3\omega_1}{2} \sqrt{1+z} e^{\frac{3\omega_1}{2} \frac{1+3\omega_0+3\omega_1}{2} \frac{1+3\omega_0-3\omega_1}{2}} \right. \\ & \times \left(\Gamma\left(-\frac{3\omega_0}{2} + \frac{3\omega_1}{2} + \frac{3}{2}, \frac{3\omega_1}{2}\right) - \Gamma\left(-\frac{3\omega_0}{2} + \frac{3\omega_1}{2} + \frac{3}{2}, \frac{3\omega_1(1+z)}{2}\right) \right) \\ & + 3(1+z)^{\frac{3\omega_0+3\omega_1}{2}} e^{-\frac{3\omega_1 z}{2}} \left(\frac{3\omega_1^2}{2} + (z-3\omega_0+2)\omega_1 + \frac{3\left(-\frac{1}{3} + \omega_0\right)^2}{2} \right) \\ & \left. + (3\omega_0 - 6\omega_1 - 1)\sqrt{1+z} \right). \end{aligned} \tag{31}$$

A more compact numerical relationship is derived with the best minimax rational approximation of degree (2, 2) for the luminosity distance, D_{L22} , on the interval in redshift [0, 2.4]

$$D_{L22} = \frac{-0.138341 + (3104.76 + 2838.17z)z}{0.745533 + (0.203583 + 0.00470683z)z}. \tag{32}$$

The above relationship can be inverted in order to have the redshift, z_{22} , as a function of the luminosity distance

$$\begin{aligned} z_{22} = & \frac{1}{4.70682 \times 10^9 D_{L22} - 2.83817 \times 10^{15}} \times 10 \left(1.01791 \times 10^{10} D_{L22} - 1.55238 \times 10^{14} \right. \\ & \left. + \sqrt{6.85244 \times 10^{19} D_{L22}^2 + 1.79991 \times 10^{25} D_{L22} + 2.41027 \times 10^{28}} \right). \end{aligned} \tag{33}$$

The derivative of the approximate luminosity distance is

$$\frac{\partial D_{L22}}{\partial z} = \frac{1.91019 \times 10^8 z + 2.54212 \times 10^7 z^2 + 1.04482 \times 10^8}{(z + 39.2133)^2 (z + 4.03927)^2}. \tag{34}$$

Figure 1 shows the difference between the analytical and the numerical relationship for the luminosity distance as a function of the redshift.

The distance modulus $\mu(z)$ has the following analytical expression

$$\mu(z) = (m - M) = 25 + \frac{5 \ln\left(\frac{(1+z)cN}{A}\right)}{\ln(10)}. \tag{35}$$

3.4. Second Model

According to [8], the EoS for the second model is

$$\omega = \omega_0 + \frac{\omega_1 z(1+z)}{z^2 + 1}, \tag{36}$$

which corresponds to

$$H(z) = (z^2 + 1)^{\frac{3\omega_1}{4}} H_0 (1+z)^{\frac{3\omega_0}{2} + \frac{3}{2}}. \tag{37}$$

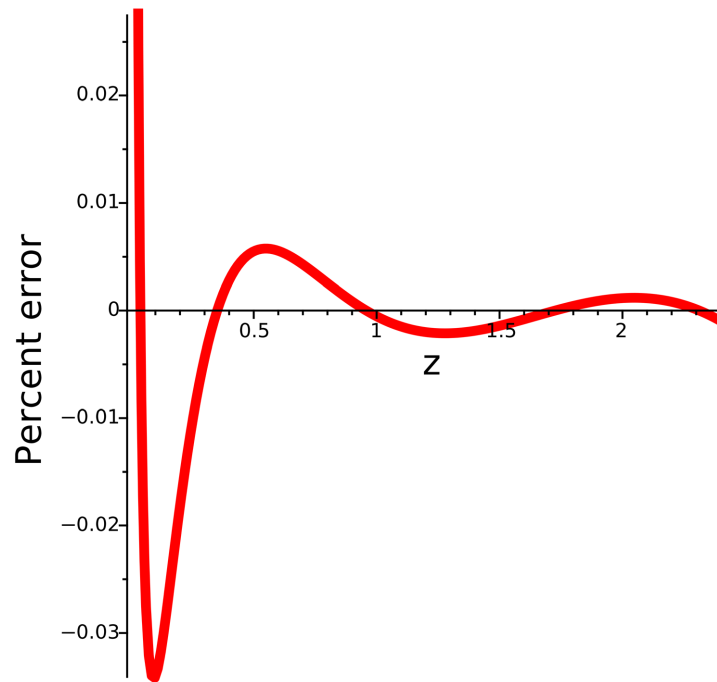


Figure 1. The percent error evaluates the discrepancy between the luminosity distance evaluated analytically, Equation (23), and that evaluated numerically, Equation (34).

In this case, the integral (22) can be evaluated but has a complicated expression and therefore we shift to the numerical analysis.

3.5. Third Model

According to [8], the EoS for the third model is

$$\omega = \omega_0 + \frac{\omega_1 z^2}{z^2 + 1}, \quad (38)$$

which corresponds to

$$H(z) = H_0 (1+z)^{\frac{3\omega_0}{2} + \frac{3\omega_1}{4} + \frac{3}{2}} (z^2 + 1)^{\frac{3\omega_1}{8}} e^{-\frac{3\omega_1 \arctan(z)}{4}}. \quad (39)$$

In this case the integral (22) cannot be evaluated and therefore we shift to the numerical analysis.

3.6. Fourth Model (New)

The fourth model (new) for the EoS is

$$\omega = z^2 \omega_1 + \omega_0, \quad (40)$$

which corresponds to

$$H(z) = (1+z)^{\frac{3\omega_0}{2} + \frac{3}{2} + \frac{3\omega_1}{2}} H_0 e^{\frac{3\omega_1 z(z-2)}{4}}. \quad (41)$$

At the moment of writing, the integral (22) cannot be evaluated. We now explore two approximations. The first approximation of $1/H(z)$ is given by the following series

$$\frac{1}{H(z)} = \frac{(1+z)^{\frac{3\omega_1}{2} \frac{3\omega_1}{2} \frac{3}{2}} \sum_{k=0}^{\infty} \frac{\left(\frac{3}{4}\right)^k (-\omega_1 (z-2)z)^k}{k!}}{H_0} \tag{42}$$

An approximate expression of order 4 for the distance modulus can be obtained by inserting the data of **Table 2**.

$$\begin{aligned} \mu(z) &= (m - M) \\ &= \frac{1}{\ln(2) + \ln(5)} \left(-25 \ln(2) + 25 \ln(5) + 5 \ln \left(-495.452 \left((49446.5 - 6.95944z^5 \right. \right. \right. \\ &\quad \left. \left. \left. + 173.172z^3 - 0.048045z^8 + 0.49566z^7 - 2.6263z^4 - 0.70507z^6 \right. \right. \right. \\ &\quad \left. \left. \left. - 3972.99z + 247.988z^2 \right) (1+z)^{0.406328} - 49446.5\sqrt{1+z} \right) \sqrt{1+z} \right). \end{aligned} \tag{43}$$

The percent error of the above distance modulus in the interval $0.01 < z < 2.4$ is shown in **Figure 2**.

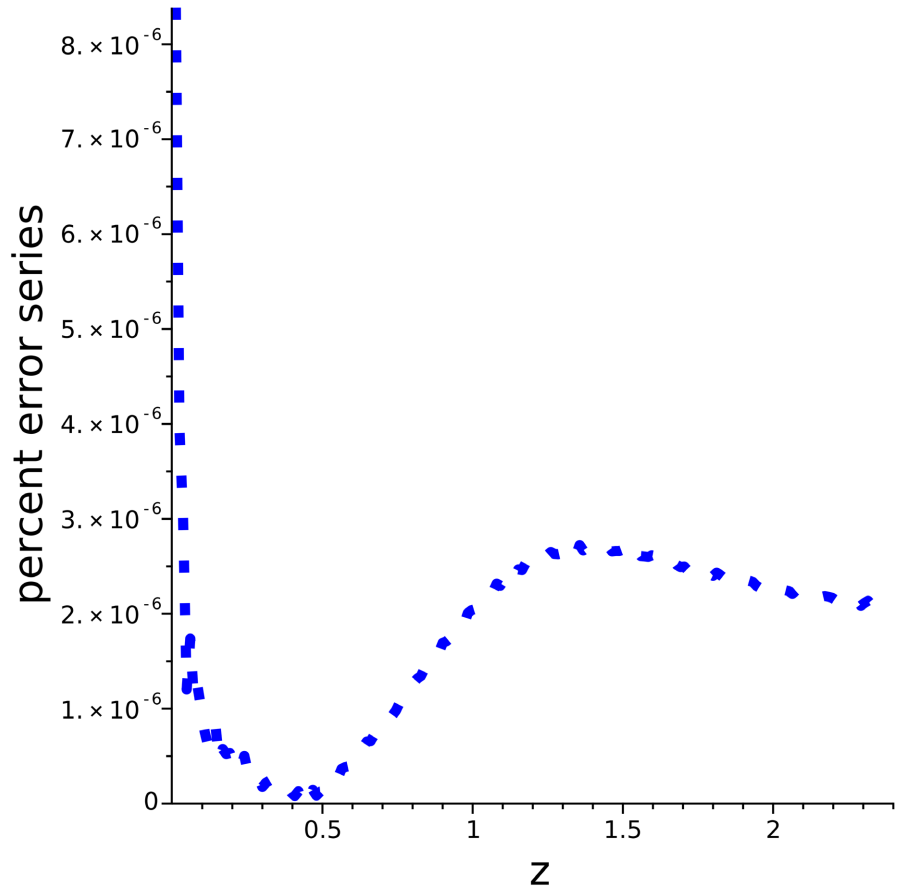


Figure 2. The percent error evaluates the discrepancy between distance modulus evaluated numerically and that evaluated through a series of order 4.

The second approximation of $1/H(z)$ is given by the Padé approximant evaluated around $z = 1$

$$\frac{1}{H(z=1)} = H_{2,1}. \quad (44)$$

A Padé approximation of the distance modulus is obtained by inserting the data of **Table 2**:

$$\begin{aligned} \mu(z)_{2,1} &= (m-M)_{2,1} \\ &= 25 + \frac{5 \ln(1300.5(1+z)(1.9229 \ln(7.2813 + 6.262z) - 3.8177 + 0.69578(-0.41053z + 2.1251)z))}{\ln(10)}. \end{aligned} \quad (45)$$

The maximum percent error of the Padé distance modulus in $0.01 < z < 2.4$ is ≈ 0.12 . In order to invert the above relationship, we first apply the minimax algorithm, which transforms the above relationship to

$$\mu(z)_{2,1} = (m-M)_{2,1} = \frac{1.89433 + (33.4185 + 1.37875z)z}{0.058972 + 0.780935z}, \quad (46)$$

from which the redshift as a function of the modulus is derived

$$z = 0.28320\mu - 12.119 + 1.4505 \times 10^{-10} \sqrt{3.8116 \times 10^{18} \mu^2 - 3.2418 \times 10^{20} \mu + 6.9146 \times 10^{21}}. \quad (47)$$

The above inverse relationship is displayed in **Figure 3**.

Inverse function

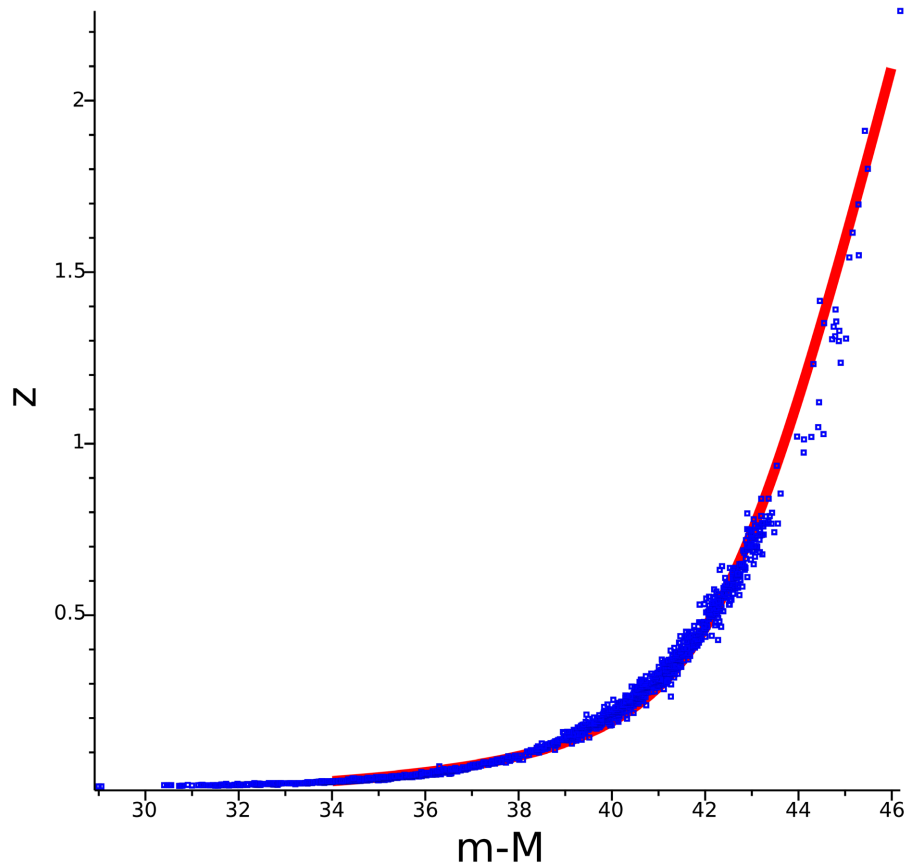


Figure 3. The redshift as a function of the distance modulus (red line) and the observed points belonging to the Pantheon+ catalog (blue squares).

3.7. Fifth Model (New)

The fifth model (new) for the EoS is

$$\omega = \omega_0 + z^3 \omega_1, \quad (48)$$

which corresponds to

$$H(z) = H(z) = (1+z)^{\frac{3\omega_0}{2} + \frac{3}{2} \frac{3\omega_1}{2}} H_0 e^{\frac{\omega_1 z(2z^2 - 3z + 6)}{4}}. \quad (49)$$

The basic integral can be approximated by adopting a series expansion around $z = 1$ up to order 4, and therefore, the luminosity distance is

$$\begin{aligned} D_L(z) &= c(1+z) \times \int_0^z \frac{dz'}{E(z')} \\ &= -\frac{1}{512} L_1 z^5 + \frac{1}{512} L_2 z^4 - \frac{1}{256} L_3 z^3 - \frac{1}{256} L_4 z^2 + \frac{1}{128} L_5 z \end{aligned} \quad (50)$$

where

$$L_1 = \frac{c(9\omega_0^3 + 27\omega_0^2\omega_1 + 27\omega_0\omega_1^2 + 9\omega_1^3 + 45\omega_0^2 - 18\omega_0\omega_1 - 63\omega_1^2 + 71\omega_0 + 11\omega_1 + 35)}{e^{\frac{3(\omega_0+1-\omega_1)\ln(2)}{2}} H_0 e^{\frac{5\omega_1}{4}}}, \quad (51a)$$

$$L_2 = \frac{c(27\omega_0^3 + 81\omega_0^2\omega_1 + 81\omega_0\omega_1^2 + 27\omega_1^3 + 183\omega_0^2 + 42\omega_0\omega_1 - 141\omega_1^2 + 341\omega_0 - 31\omega_1 + 185)}{e^{\frac{3(\omega_0+1-\omega_1)\ln(2)}{2}} H_0 e^{\frac{5\omega_1}{4}}}, \quad (51b)$$

$$L_3 = \frac{c(9\omega_0^3 + 27\omega_0^2\omega_1 + 27\omega_0\omega_1^2 + 9\omega_1^3 + 93\omega_0^2 + 78\omega_0\omega_1 - 15\omega_1^2 + 295\omega_0 + 43\omega_1 + 211)}{e^{\frac{3(\omega_0+1-\omega_1)\ln(2)}{2}} H_0 e^{\frac{5\omega_1}{4}}}, \quad (51c)$$

$$L_4 = \frac{c(9\omega_0^3 + 27\omega_0^2\omega_1 + 27\omega_0\omega_1^2 + 9\omega_1^3 + 45\omega_0^2 - 18\omega_0\omega_1 - 63\omega_1^2 - 25\omega_0 - 85\omega_1 - 317)}{e^{\frac{3(\omega_0+1-\omega_1)\ln(2)}{2}} H_0 e^{\frac{5\omega_1}{4}}}, \quad (51d)$$

$$L_5 = \frac{c(9\omega_0^3 + 27\omega_0^2\omega_1 + 27\omega_0\omega_1^2 + 9\omega_1^3 + 81\omega_0^2 + 54\omega_0\omega_1 - 27\omega_1^2 + 263\omega_0 + 59\omega_1 + 319)}{e^{\frac{3(\omega_0+1-\omega_1)\ln(2)}{2}} H_0 e^{\frac{5\omega_1}{4}}}. \quad (51e)$$

An approximate distance modulus is now easily derived using Equation (24) and the parameters of **Table 2**

$$\begin{aligned} \mu(z) &= (m - M) \\ &= 25 + \frac{5 \ln \left(\frac{24.6562(1+z)(-212.831z + 56.2073z^2 - 13.1375z^3 + 2.95741z^4)}{e^{0.412976\ln(2)}} \right)}{\ln(10)}. \end{aligned} \quad (52)$$

The percent error of the above distance modulus in the interval $0.01 < z < 2.4$ is given in **Figure 4**.

3.8. Sixth Model (New)

The sixth model (new) for the EoS is

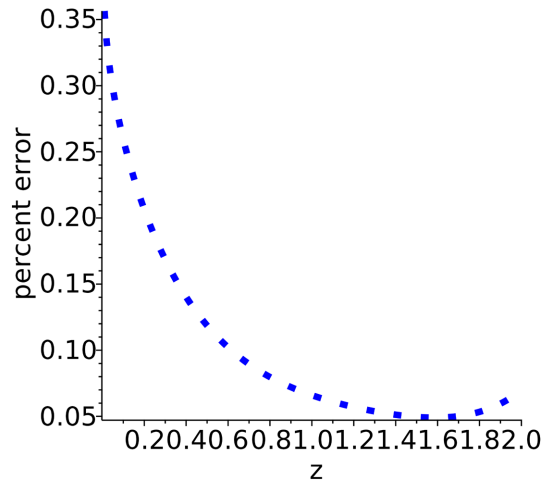


Figure 4. The percent error evaluates the discrepancy between distance modulus for the fifth model evaluated numerically and that evaluated through a series of order 4, see Equation (52).

$$\omega = \omega_0 + \frac{\omega_1 z^3}{z^3 + 1}, \tag{53}$$

which corresponds to

$$H(z) = H_0 (z^2 - z + 1)^{\frac{\omega_1}{4}} (1+z)^{\frac{3\omega_0}{2} + \omega_1 + \frac{3}{2}} e^{-\frac{\omega_1 \left(6\sqrt{3}(1+z) \arctan\left(\frac{(2z-1)\sqrt{3}}{3}\right) + \pi(1+z)\sqrt{3} + 18z \right)}{36+36z}}. \tag{54}$$

Also here the basic integral is approximated by a series expansion around $z = 1$ up to order 3. Therefore the luminosity distance is

$$D_L(z) = 25 + \frac{5 \ln\left(\frac{1}{128} L_1 z^4 - \frac{1}{64} L_2 z^3 + \frac{1}{16} L_3 z^2 + \frac{1}{128} L_4 z\right)}{\ln(10)}, \tag{55}$$

where

$$L_1 = \frac{c(12\omega_0^2 + 12\omega_0\omega_1 + 3\omega_1^2 + 32\omega_0 + 4\omega_1 + 20)}{H_0 e^{\frac{(3+2\omega_1+3\omega_0)\ln(2)}{2}} e^{-\frac{\sqrt{3}(2\pi+3\sqrt{3})\omega_1}{36}}}, \tag{56a}$$

$$L_2 = \frac{c(12\omega_0^2 + 12\omega_0\omega_1 + 3\omega_1^2 + 56\omega_0 + 16\omega_1 + 44)}{H_0 e^{\frac{(3+2\omega_1+3\omega_0)\ln(2)}{2}} e^{-\frac{\sqrt{3}(2\pi+3\sqrt{3})\omega_1}{36}}}, \tag{56b}$$

$$L_3 = \frac{c(6\omega_0 + 3\omega_1 + 22)}{H_0 e^{\frac{(3+2\omega_1+3\omega_0)\ln(2)}{2}} e^{-\frac{\sqrt{3}(2\pi+3\sqrt{3})\omega_1}{36}}}, \tag{56c}$$

$$L_4 = \frac{c(36\omega_0^2 + 36\omega_0\omega_1 + 9\omega_1^2 + 192\omega_0 + 60\omega_1 + 284)}{H_0 e^{\frac{(3+2\omega_1+3\omega_0)\ln(2)}{2}} e^{-\frac{\sqrt{3}(2\pi+3\sqrt{3})\omega_1}{36}}}. \tag{56d}$$

The distance modulus is now easily derived using Equation (24)

$$\begin{aligned} \mu(z) &= (m - M) \\ &= 25 + \frac{5 \ln \left(-\frac{1}{4096} L_1 z^5 + \frac{1}{4096} L_2 z^4 - \frac{1}{2048} L_3 z^3 - \frac{1}{2048} L_4 z^2 + \frac{1}{1024} L_5 z \right)}{\ln(10)}. \end{aligned} \quad (57)$$

A numerical expression for the distance modulus is derived using the parameters of **Table 2**

$$\mu(z) = 25 + \frac{5 \ln \left(\frac{32.5588(1+z)(6.6977z^3 - 50.198z^2 + 208.302z)}{e^{1.0041 \ln(2)} e^{-0.00703688\sqrt{3}(2\pi+3\sqrt{3})}} \right)}{\ln(10)}. \quad (58)$$

The percent error of the above distance modulus in the interval $0.01 < z < 2.4$ is given in **Figure 5**.

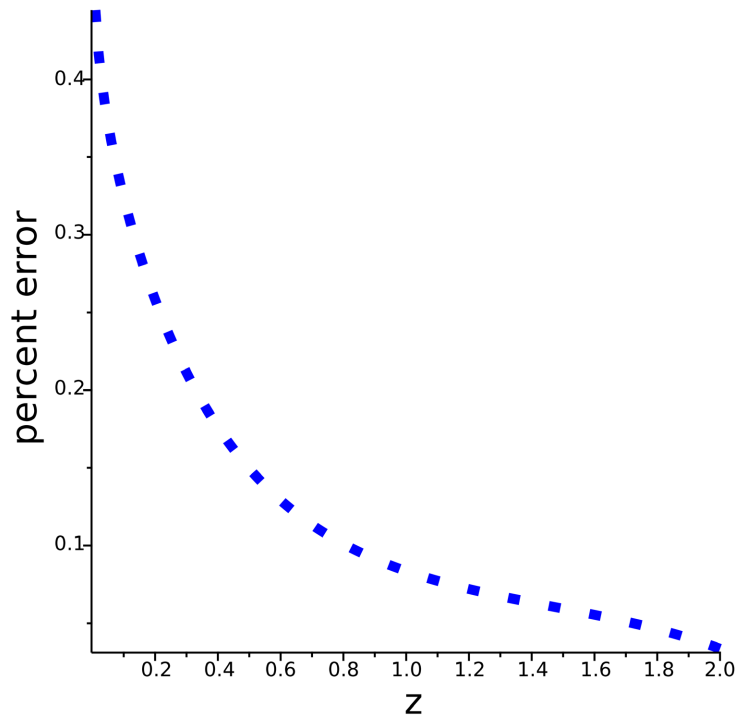


Figure 5. The percent error evaluates the discrepancy between the distance modulus for the sixth model evaluated numerically and that evaluated through a series of order 3, see Equation (58).

4. Astrophysical Application

We review the adopted statistics and present the derivation of the best fit parameters for the distance modulus of SNs. The catalog analysed is the Pantheon+, which contains 1701 distance moduli of supernovae (SNe) Ia, the error on the distance modulus and the redshift [6].

4.1. The Adopted Statistics

In the case of the distance modulus, the merit function χ^2 is

$$\chi^2 = \sum_{i=1}^N \left[\frac{(m-M)_i - (m-M)(z_i)_{th}}{\sigma_i} \right]^2, \quad (59)$$

where N is the number of SNs, $(m-M)_i$ is the observed distance modulus evaluated at a redshift of z_i , σ_i is the error in the observed distance modulus evaluated at z_i , and $(m-M)(z_i)_{th}$ is the theoretical distance modulus evaluated at z_i , see formula (15.5.5) in [20]. The reduced merit function χ_{red}^2 is

$$\chi_{red}^2 = \chi^2 / NF, \quad (60)$$

where $NF = N - k$ is the number of degrees of freedom, N is the number of SNs, and k is the number of free parameters. Another useful statistical parameter is the associated Q -value, which has to be understood as the maximum probability of obtaining a better fitting, see formula (15.2.12) in [20]:

$$Q = 1 - \text{GAMMQ} \left(\frac{N-k}{2}, \frac{\chi^2}{2} \right), \quad (61)$$

where GAMMQ is a subroutine for the incomplete gamma function. The Akaike information criterion (AIC), see [21], is defined by

$$\text{AIC} = 2k - 2 \ln(L), \quad (62)$$

where L is the likelihood function. We assume a Gaussian distribution for the errors; then the likelihood function can be derived from the χ^2 statistic

$$L \propto \exp \left(-\frac{\chi^2}{2} \right) \text{ where } \chi^2 \text{ has been computed by Equation chi-square), see$$

[22] [23]. Now the AIC becomes

$$\text{AIC} = 2k + \chi^2. \quad (63)$$

The goodness of the approximation in evaluating a physical variable p is evaluated by the percentage error δ

$$\delta = \frac{|p - p_{approx}|}{p} \times 100, \quad (64)$$

where p_{approx} is an approximation of p .

4.2. The Distance Modulus

The cosmological parameters of the two cosmologies of reference are given in **Table 1**; the six models of the $f(Q, L_m)$ gravity model are given in **Table 2**.

Table 1. Numerical values of χ^2 , χ_{red}^2 , Q and the AIC of the Hubble diagram for the Pantheon+ sample, k stands for the number of parameters, H_0 is expressed in $\text{km} \cdot \text{s}^{-1} \cdot \text{Mpc}^{-1}$; 1701 SN Ia. Case of standard cosmologies.

cosmology	equation	k	parameters	χ^2	χ_{red}^2	Q	AIC
Λ CDM	(11)	3	$H_0 = (72.33 \pm 0.15)$; $\Omega_M = (0.331 \pm 0.02)$; $\Omega_\Lambda = (0.56 \pm 0.02)$	810.68	0.47	1	816.68
wCDM	(21)	3	$H_0 = (72.15 \pm 0.28)$; $\Omega_M = (0.217 \pm 0.0094)$; $w = (-0.701 \pm 0.017)$	809.65	0.47	1	815.65

Table 2. Numerical values of χ^2 , χ_{red}^2 , Q and the AIC of the Hubble diagram for the Pantheon+ sample, k stands for the number of parameters, H_0 is expressed in $\text{km}\cdot\text{s}^{-1}\cdot\text{Mpc}^{-1}$; 1701 SN Ia. Case of $f(Q, L_m)$ gravity model.

cosmology equation	k	parameters	χ^2	χ_{red}^2	Q	AIC
model 1 (35)	3	$H_0 = (72.08 \pm 0.32)$; $\omega_0 = (-0.532 \pm 0.02)$; $\omega_1 = (0.190 \pm 0.008)$	809.72	0.476	1	815.72
model 2 (24)	3	$H_0 = (72.07 \pm 0.27)$; $\omega_0 = (-0.536 \pm 0.03)$; $\omega_1 = (0.184 \pm 0.09)$	809.73	0.476	1	815.73
model 3 (24)	3	$H_0 = (72.07 \pm 0.27)$; $\omega_0 = (-0.524 \pm 0.02)$; $\omega_1 = (0.533 \pm 0.02)$	809.69	0.476	1	815.69
model 4 (24)	3	$H_0 = (72 \pm 0.26)$; $\omega_0 = (-0.511 \pm 0.02)$; $\omega_1 = (0.24 \pm 0.149)$	809.66	0.476	1	815.66
model 5 (24)	3	$H_0 = (71.96 \pm 0.26)$; $\omega_0 = (-0.502 \pm 0.02)$; $\omega_1 = (0.222 \pm 0.163)$	809.79	0.476	1	815.79
model 6 (24)	3	$H_0 = (71.93 \pm 0.262)$; $\omega_0 = (-0.499 \pm 0.02)$; $\omega_1 = (0.253 \pm 0.265)$	810.25	0.477	1	816.25

Figure 6 shows the best fit in the Λ CDM cosmology for the Pantheon+ compilation.

The different behaviors of some of the cosmologies here analysed is evident when high values of the redshift are considered, for example the interval $[2, 2.4]$, see **Figure 7**.

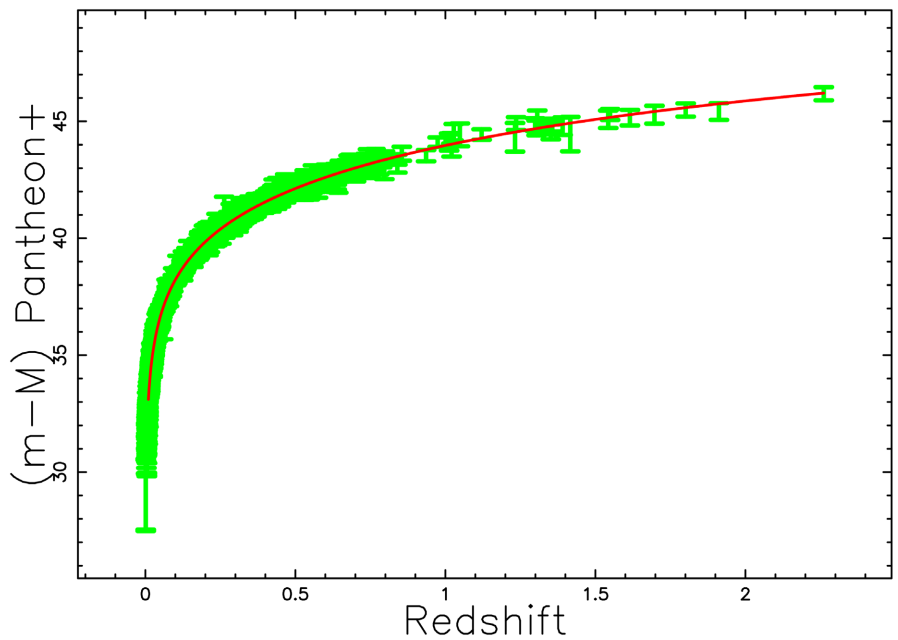


Figure 6. Hubble diagram for the Pantheon+ sample, green points with error bars. The solid red line represents the best fit for the distance modulus in model 1 for $f(Q, L_m)$ cosmology. The theoretical uncertainties are represented through green vertical lines. The parameters are as in the first line of **Table 2**.

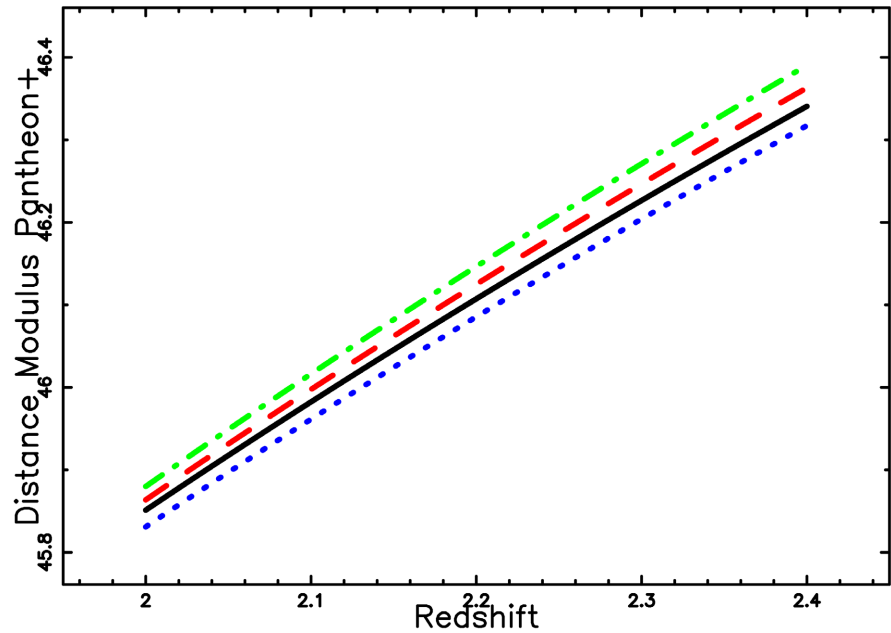


Figure 7. Hubble diagram for the Λ CDM cosmology, black full line, model 1 for $f(Q, L_m)$ cosmology, red dashed line, model 2 for w CDM cosmology, green dot-dash-dot-dash line and model 3 for $f(Q, L_m)$ cosmology, blue dotted line. The parameters are in [Table 1](#) and [Table 2](#).

5. The Photometric Maximum

We review the processed data, the Schechter luminosity function and the theory which models the number of galaxies as a function of the redshift.

5.1. The SDSS Data

We processed the SDSS Photometric Catalogue DR 12, see [\[24\]](#), which contains 10450256 galaxies (elliptical + spiral) with redshifts. In the following, we will use the generic term “galaxy” without distinguishing between the two types, elliptical and spiral.

5.2. Luminosity Function for Galaxies

We used the Schechter function, see [\[25\]](#), as a luminosity function (LF) for galaxies

$$\Phi(L)dL = \left(\frac{\Phi^*}{L^*}\right) \left(\frac{L}{L^*}\right)^\alpha \exp\left(-\frac{L}{L^*}\right) dL, \quad (65)$$

here α sets the slope for low values of luminosity, L , L^* is the characteristic luminosity and Φ^* is the normalisation. The equivalent distribution in absolute magnitude is

$$\Phi(M)dM = 0.921\Phi^* 10^{0.4(\alpha+1)(M^*-M)} \exp\left(-10^{0.4(M^*-M)}\right) dM, \quad (66)$$

where M^* is the characteristic magnitude as derived from the data. The scaling

with h is $M^* - 5 \log_{10} h$ and $\Phi^* h^3 [\text{Mpc}^{-3}]$.

5.3. The Theory

The flux density or irradiance, f , is

$$f = \frac{L}{4\pi r^2}, \quad (67)$$

where r is the luminosity distance. The flux density in SI units is expressed in Watt/m² and in astrophysical units in L_{\odot}/Mpc^2 . The luminosity distance is

$$r = D_{L22}, \quad (68)$$

see Equation (32) and the relationship between dr and dz is

$$\frac{dr}{dz} = \frac{\partial D_{L22}}{\partial z}, \quad (69)$$

see Equation (34).

The joint distribution in z and f for the number of galaxies, see formula (5.133) in [9] or formula (1.104) in [26] or formula (1.117) in [27], is

$$\frac{dN}{d\Omega dz df} = \frac{1}{4\pi} \int_0^{\infty} 4\pi r^2 dr \Phi(L; L^*, \sigma) \delta(z - (z_{22})) \delta\left(f - \frac{L}{4\pi r^2}\right), \quad (70)$$

where δ is the Dirac delta function, $\Phi(L; L^*, \sigma)$ has been defined in Equation (65) and z_{22} has been defined in Equation (33). An explicit version is

$$\frac{dN}{d\Omega dz df} = \frac{NN}{DD}, \quad (71)$$

where

$$\begin{aligned} NN &= 567218 \left(-0.138330 + 3104.76z + 2838.17z^2 \right)^4 \\ &\times \left(\frac{4\pi f \left(-0.138330 + (3104.76 + 2838.17z)z \right)^2}{\left((0.745533 + (0.203583 + 0.00470684z)z \right)^2 L^*} \right)^{\alpha} \\ &\times e^{\frac{4\pi f \left(-0.138330 + (3104.76 + 2838.17z)z \right)^2}{\left((0.745533 + (0.203583 + 0.00470684z)z \right)^2 L^*}} \times \Phi^* \left(4231.9z + 563.19z^2 + 2314.73 \right), \end{aligned} \quad (72)$$

and

$$DD = \left(0.745533 + 0.203583z + 0.00470684z^2 \right)^4 L^* (z + 39.2133)^2 (z + 4.03927)^2. \quad (73)$$

The total number of galaxies comprised between a minimum value of flux, f_{\min} , and a maximum value of flux, f_{\max} , can be computed through the integral

$$\frac{dN}{d\Omega dz} = \int_{f_{\min}}^{f_{\max}} \frac{NN}{DD} df. \quad (74)$$

This integral has a complicated analytical solution in terms of the Whittaker function $M_{\kappa, \mu}(z)$, see [18]. **Figure 8** presents all of the galaxies of SDSS DR12 and also the theoretical curve.

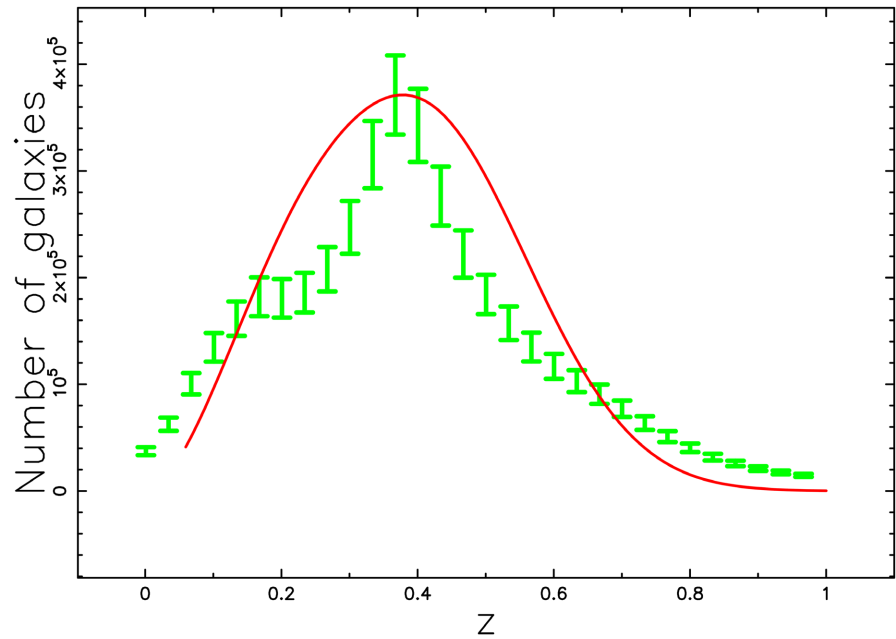


Figure 8. The galaxies of SDSS DR 12 (u-band) with $1.27 \times 10^{-21} \text{ Watt/m}^2 \leq f \leq 1.59 \times 10^{-16} \text{ Watt/m}^2$ or $400 L_{\odot}/\text{Mpc}^2 \leq f \leq 5 \times 10^7 L_{\odot}/\text{Mpc}^2$ are organized by frequencies versus redshift and the error bar is given by the square root of the frequency (green errors). The maximum frequency of the observed galaxies is at $z = 0.38$. The full line is the theoretical curve that is generated by $\frac{dN}{d\Omega dr df}$ as given by the application of the Schechter LF, which is Equation (71), red line, and the theoretical maximum is at $z = 0.382$. The parameters of the Schechter LF are $L^* = 1.75 \times 10^{10} L_{\odot}$, $\Phi^* = 0.03 \text{ Mpc}^{-3}$ and $\alpha = -0.9$.

6. Conclusions

Cosmologies. The $f(Q, C)$ gravity here presented in three new plus three existing models performs quite well in respect to the standard cosmologies of reference. **Table 3** presents the results in order of increasing χ^2 ; the winner is the Λ CDM cosmology followed by the $f(Q, C)$ gravity model 4.

Table 3. Increasing values of χ^2 for the cosmologies here presented.

number	cosmology	χ^2
1	wCDM	809.654
2	gravity model 4	809.662
3	gravity model 3	809.697
4	gravity model 1	809.725
5	gravity model 2	809.736
6	gravity model 5	809.794
7	gravity model 6	810.255
8	Λ CDM	810.689

The number of galaxies. The theoretical number of galaxies versus the redshift can be parametrized in the framework of the $f(Q, C)$ gravity as a function of the observed flux, see Equation (70). The new derived formula for all the galaxies as a function of the redshift has been applied to the SDSS DR 12 catalog, see **Figure 8**.

Conflicts of Interest

The author declares no conflicts of interest regarding the publication of this paper.

References

- [1] Riess, A.G., Filippenko, A.V., Challis, P., Clocchiatti, A., Diercks, A., Garnavich, P.M., *et al.* (1998) Observational Evidence from Supernovae for an Accelerating Universe and a Cosmological Constant. *The Astronomical Journal*, **116**, 1009-1038. <https://doi.org/10.1086/300499>
- [2] Suzuki, N., Rubin, D., Lidman, C., Aldering, G., Amanullah, R., Barbary, K., *et al.* (2012) The Hubble Space Telescope Cluster Supernova Survey. V. Improving the Dark-Energy Constraints above $z > 1$ and Building an Early-Type-Hosted Supernova Sample. *The Astrophysical Journal*, **746**, Article 85. <https://doi.org/10.1088/0004-637x/746/1/85>
- [3] Betoule, M., Kessler, R., Guy, J. and Mosher, J. (2014) Improved Cosmological Constraints from a Joint Analysis of the SDSS-II and SNLS Supernova Samples. *Astronomy & Astrophysics*, **568**, A22.
- [4] Jones, D.O., Scolnic, D.M., Riess, A.G., Rest, A., Kirshner, R.P., Berger, E., *et al.* (2018) Measuring Dark Energy Properties with Photometrically Classified Pan-Starrs Supernovae. II. Cosmological Parameters. *The Astrophysical Journal*, **857**, Article 51. <https://doi.org/10.3847/1538-4357/aab6b1>
- [5] Scolnic, D.M., Jones, D.O., Rest, A., Pan, Y.C., Chornock, R., Foley, R.J., *et al.* (2018) The Complete Light-Curve Sample of Spectroscopically Confirmed SNe Ia from Pan-STARRS1 and Cosmological Constraints from the Combined Pantheon Sample. *The Astrophysical Journal*, **859**, Article 101. <https://doi.org/10.3847/1538-4357/aab9bb>
- [6] Brout, D., Scolnic, D., Popovic, B., *et al.* (2022) The Pantheon+ Analysis: Cosmological Constraints. *The Astrophysical Journal*, **938**, Article 110.
- [7] Samaddar, A., Singh, S.S., Muhammad, S. and Zotos, E.E. (2024) Behaviours of Rip Cosmological Models in $f(q, c)$ Gravity. *Nuclear Physics B*, **1006**, Article ID: 116643. <https://doi.org/10.1016/j.nuclphysb.2024.116643>
- [8] Samaddar, A. and Surendra Singh, S. (2024) Constraining Model Parameters in $f(Q, C)$ Gravity: Observational Analysis and Geometric Diagnostics. arXiv: 2411.17754.
- [9] Peebles, P.J.E. (1993) Principles of Physical Cosmology. Princeton University Press.
- [10] Zaninetti, L. (2021) Sparse Formulae for the Distance Modulus in Cosmology. *Journal of High Energy Physics, Gravitation and Cosmology*, **7**, 965-992. <https://doi.org/10.4236/jhepgc.2021.73057>
- [11] Turner, M.S. and White, M. (1997) CDM Models with a Smooth Component. *Physical Review D*, **56**, R4439-R4443. <https://doi.org/10.1103/physrevd.56.r4439>
- [12] Tripathi, A., Sangwan, A. and Jassal, H.K. (2017) Dark Energy Equation of State Parameter and Its Evolution at Low Redshift. *Journal of Cosmology and Astroparticle Physics*, **2017**, Article 12. <https://doi.org/10.1088/1475-7516/2017/06/012>

-
- [13] Wei, J., Ma, Q. and Wu, X. (2015) Utilizing the Updated Gamma-Ray Bursts and Type Ia Supernovae to Constrain the Cardassian Expansion Model and Dark Energy. *Advances in Astronomy*, **2015**, Article ID: 576093. <https://doi.org/10.1155/2015/576093>
- [14] Abramowitz, M., Stegun, I.A. and Romain, J.E. (1966) Handbook of Mathematical Functions, with Formulas, Graphs, and Mathematical Tables. *Physics Today*, **19**, 120-121. <https://doi.org/10.1063/1.3047921>
- [15] von Seggern, D. (1992) CRC Standard Curves and Surfaces. CRC Press.
- [16] Thompson, W.J. (1997) Atlas for Computing Mathematical Functions. Wiley.
- [17] Gradshteyn, I.S., Ryzhik, I.M., Jeffrey, A. and Zwillinger, D. (2007) Table of Integrals, Series, and Products. Academic Press.
- [18] Olver, F.W.J., Lozier, D.W., Boisvert, R.F. and Clark, C.W. (2010) NIST Handbook of Mathematical Functions. Cambridge University Press.
- [19] Zaninetti, L. (2019) The Distance Modulus in Dark Energy and Cardassian Cosmologies via the Hypergeometric Function. *International Journal of Astronomy and Astrophysics*, **9**, 231-246. <https://doi.org/10.4236/ijaa.2019.93017>
- [20] Press, W.H., Teukolsky, S.A., Vetterling, W.T. and Flannery, B.P. (1992) Numerical Recipes in FORTRAN: The Art of Scientific Computing. Cambridge University Press.
- [21] Akaike, H. (1974) A New Look at the Statistical Model Identification. *IEEE Transactions on Automatic Control*, **19**, 716-723. <https://doi.org/10.1109/tac.1974.1100705>
- [22] Liddle, A.R. (2004) How Many Cosmological Parameters? *Monthly Notices of the Royal Astronomical Society*, **351**, L49-L53. <https://doi.org/10.1111/j.1365-2966.2004.08033.x>
- [23] Godlowski, W. and Szydowski, M. (2005) Constraints on Dark Energy Models from Supernovae. In: Turatto, M., Benetti, S., Zampieri, L. and Shea, W., Eds., 1604-2004: *Supernovae as Cosmological Lighthouses*, Astronomical Society of the Pacific, 508-516.
- [24] Alam, S., Albareti, F.D., Allende Prieto, C., *et al.* (2015) The Eleventh and Twelfth Data Releases of the Sloan Digital Sky Survey: Final Data from SDSS-III. *The Astrophysical Journal Supplement*, **219**, Article 12.
- [25] Schechter, P. (1976) An Analytic Expression for the Luminosity Function for Galaxies. *The Astrophysical Journal*, **203**, Article 297. <https://doi.org/10.1086/154079>
- [26] Padmanabhan, T. (1996) *Cosmology and Astrophysics through Problems*. Cambridge University Press.
- [27] Padmanabhan, P. (2002) *Theoretical Astrophysics. Vol. III: Galaxies and Cosmology*. Cambridge University Press.